Molecular Orientation and Optical Anisotropy in Drawn Films of Miscible Blends Composed of Cellulose Acetate and Poly(*N*-vinylpyrrolidone-*co*-methyl methacrylate)

Takahiro Ohno and Yoshiyuki Nishio*

Division of Forest and Biomaterials Science, Graduate School of Agriculture, Kyoto University, Kyoto 606-8502, Japan

Received December 20, 2006; Revised Manuscript Received March 7, 2007

ABSTRACT: Poly(*N*-vinylpyrrolidone) (PVP) is miscible with cellulose acetate (CA) with a degree of acetyl substitution (DS) of less than ca. 2.75, and a random copolymer of *N*-vinylpyrrolidone (VP) and methyl methacrylate (MMA) can also form completely miscible blends with CA, when the VP fraction in the copolymer is >30 mol % and the DS of CA is ≤2.5. The molecular orientation and optical anisotropy induced by uniaxial deformation of the miscible blends of the VP-containing vinyl polymers [P(VP-*co*-MMA)s] with CA were characterized by a fluorescence polarization method and birefringence quantification, respectively. Film samples of more than 10 pairs of CA/P(VP-*co*-MMA) were cast from mixed polymer solutions in *N*,*N*-dimethylformamide containing a slight amount of a stilbene derivative as a fluorescent probe, to assume different blend compositions for each individual polymer pair. Through analysis of polarized fluorescence intensity, it was found that all the drawn films gave a positive orientation function, but the orientation development became suppressed with increasing content of the vinyl polymer component. In comparison between different CA/PVP series, the drawn blends comprising a CA of comparatively lower DS and a PVP of higher molecular weight indicated a higher degree of orientation at any stage of elongation. The molecular orientation in CA/VP−MMA copolymer blends was affected by the DS of CA in a similar manner to that in the CA/PVP series, but the VP:MMA ratio in the copolymer was less effective. The optical birefringence of the drawn films, when compared at a given draw ratio for a series of blends, decreased drastically with an increase in the vinyl polymer content and changed from positive to negative values at a certain blend composition. This optical behavior is interpretable in terms of an effect of birefringence compensation due to the positive and negative contributions of oriented CA and vinyl polymer, respectively, to the overall birefringence. The critical binary composition where the blend remains a birefringence-free material shifted to the CA-rich composition side with increasing DS of the CA used as well as with increasing VP fraction in the P(VP-*co*-MMA) component. At vinyl polymer-rich compositions, the negative birefringence observed for the drawn blends was even greater in absolute value than that of the drawn, unblended vinyl polymer, suggesting that the two constituent polymers can orient cooperatively as a result of their high miscibility.

Introduction

Polymer chains are often oriented in the process of the polymer into some industrial products whether a manufacturer intends it or not. Physical properties of the products can change sensitively according to the state of the orientation furnished. Therefore, it is important to clarify and comprehend the relationship between the molecular orientation and the physical properties such as mechanical and optical ones. In recent optical technologies, birefringence-free polymer materials that give rise to no birefringence even though the molecular orientation is induced by deformation, and, conversely, widely birefringence-controllable polymer materials as well, have been demanded to produce polarization-protecting or regulating films for liquid crystal displays[1,2] and to design other optically functional media for many-faceted prospective applications.

Several methods have so far been proposed to create the birefringence-free materials. They are the random copolymerization method,[3,4] the anisotropic molecule dopant method,[5,6] the birefringent crystal dopant method,[7,8] and the polymer blending method.[9−13] A conception common to these methods is to offset the optical anisotropy of a host component by conjugating the guest constituent providing opposite birefringence to the host. In particular, the polymer blending method may be a convenient one not only to obtain the birefringence-free material but also to acquire an additional, novel or wide-ranging property allowing the material to be used in different fields. However, there were few reports on the polymer blending method in the past decade, for most polymer pairs make no strong, attractive intermolecular interaction and rather phase-separate on a scale of more than several tens of nanometers, often leading to scattering of visible light. Therefore, a high level of miscibility at the molecular level, carried through a specific attractive force such as hydrogen-bonding or ionic interactions, would be usually required for the polymer blends to serve as optical media.

Meanwhile, cellulose and related polysaccharides have recently been reevaluated as fascinating chemicals or materials with industrially higher potential, not only due to their conformability to the environment but also due to their useful characteristics at the molecular and supramolecular levels. As a part of studies on modern applications of polysaccharides, the authors' group has been trying to design and fabricate novel multicompositional polymer materials based on cellulosics.[14,15] Cellulose acetate (CA) used in the present work is an important cellulose ester derivative established already for practical applications. For instance, it is utilized in film form due to desirable physical properties involving good optical clarity as well as in fiber form due to a comparatively high modulus and flexural and tensile strengths. In addition, CAs with a degree

* Author for correspondence: e-mail ynishio@kais.kyoto-u.ac.jp; phone +81-75-753-6250; fax +81-75-753-6300.

10.1021/ma062920t CCC: $37.00
Published on Web 03/29/2007

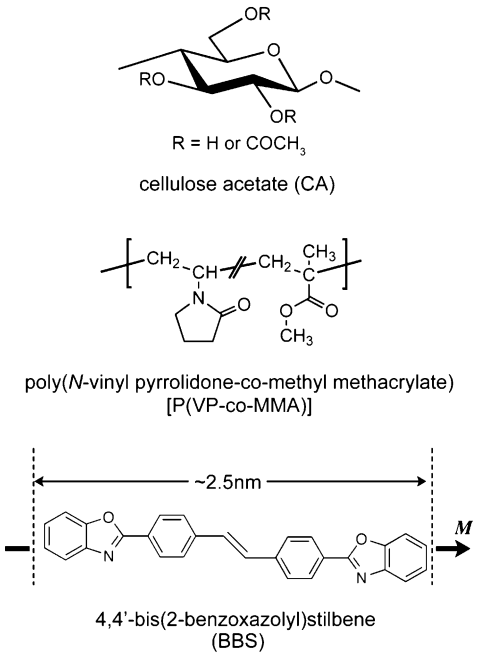

Figure 1. Structural formulas of CA, P(VP-*co*-MMA), and BBS.

of acetyl substitution (DS) of ≤2.5 have been reported to be practically biodegradable.[16−18] In order to further exploit the properties and extend the availability of CA, we have designed and characterized several CA-based hybrid materials produced by the graft copolymerization[19−22] or miscible blending with other polymers.[23−27]

In a recent paper,[27] the authors reported on the miscibility and intermolecular interactions for CA blends with synthetic homopolymers and random copolymers comprising *N*-vinylpyrrolidone (VP) and/or methyl methacrylate (MMA) units, i.e., poly(*N*-vinylpyrrolidone) (PVP), poly(methyl methacrylate) (PMMA), and poly(*N*-vinylpyrrolidone-*co*-methyl methacrylate) [P(VP-*co*-MMA)] (Figure 1). The incorporation of MMA into the vinyl polymer as a counterpart of the CA blends may be significant in practice because PMMA is an essential material in optical and medical fields on account of the distingue physical properties and safety for living bodies. On the basis of thermal analysis data, a miscibility map was constructed as a function of the DS of CA and the VP fraction in P(VP-*co*-MMA), as summarized in Figure 2. As can be seen from the map, most of the pairs composed of CA of DS ≤ 2.5 and P(VP-*co*-MMA) of VP > 30 mol % were miscible, whereas the other combinations of DS and VP values led to an immiscible blend series, but with a possible exception such as a miscible pair of DS = 2.70 and VP = 100 mol %. Fourier transform infrared (FT-IR) and solid-state ^{13}C NMR spectroscopy revealed that a driving force for the miscibility attainment was the hydrogen bonding formed between the residual hydroxyl groups of CA and the carbonyl groups of VP residues in the vinyl polymer component. The homogeneity of the miscible CA/P(VP-*co*-MMA) blends was also confirmed to be substantially on a scale within a few nanometers, through evaluations of proton spin−lattice relaxation times ($T_{1\rho}^{H}$) in the NMR study.

The present study is an extension of the blend study on the CA/P(VP-*co*-MMA) system. This blend system has a potential as optical materials of that kind stated in the beginning, in addition to the utility as membranes showing a selective liquid- or vapor-absorption property controllable by varying the blend and copolymer compositions. From such a viewpoint of functional development, therefore, we provide insight into the molecular orientation and optical behavior observed when the CA/vinyl polymer blends are mechanically deformed at elevated temperatures, in connection with the miscibility and intermolecular interaction between the two components. A fluorescence polarization technique is used to obtain information about the degree and type of molecular orientation in uniaxially drawn films of the miscible blends, and birefringence quantification is also carried out to estimate the state of optical anisotropy induced therein.

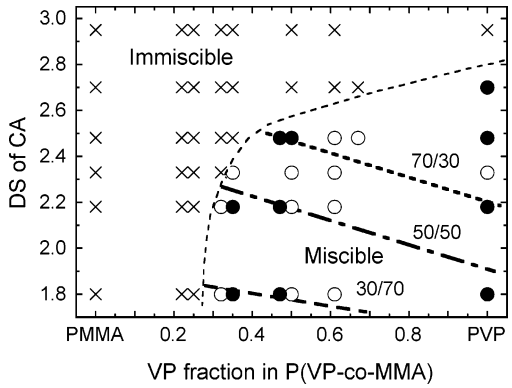

Figure 2. Miscibility map for CA/P(VP-*co*-MMA) blend series, quoted from a previous paper[27] with additional data. Symbols indicate whether a give pair of CA/P(VP-*co*-MMA) is miscible (○ and ●) or immiscible (×). Filled circles represent the blend series used in the present orientation study. Three lines, designated as 70/30, 50/50, and 30/70, inform a critical blend composition. The miscible polymer combinations fitting the respective lines can produce a birefringence-free material at the indicated critical composition (see the latter half of text for discussion).

Experimental Section

Materials. Four grades of cellulose acetate (CA), determined as DS = 1.80, 2.18, 2.48, and 2.70 by ^{1}H NMR measurements, were used in this work. The weight-average and number-average degrees of polymerization of the CAs are respectively 500−850 and 220−270,[24,27] the data of the same class being in a range of magnitude comparable to each other. The basic characterization for the respective CA samples has been described in a preceding paper.[27] Two samples of poly(*N*-vinylpyrrolidone) (PVP) differing in molecular weight (M_w) from each other, i.e., nominally M_w = 360 000 (PVP-H) and 24 500 (PVP-L), were purchased from Nacalai Tesque, Inc. Three random copolymers of poly(*N*-vinylpyrrolidone-*co*-methyl methacrylate) [P(VP-*co*-MMA)] were prepared by free radical polymerization in our laboratory,[27] the VP:MMA compositions being determined as 50:50, 47:53, and 35:65 by the FT-IR method.[28] The weight-average molecular weights of the respective copolymers were $M_w = 1.84 \times 10^5$, 2.41×10^5, and 2.90×10^5, determined by gel permeation chromatography (mobile phase, 10 mM/L lithium bromide/*N*,*N*-dimethylformamide (DMF) at 40 °C) in comparison with polystyrene standards. A fluorescent molecule, 4,4′-bis(2-benzoxazolyl)stilbene (BBS), the chemical structure of which is shown in Figure 1, was used as a probe for the orientation estimation by a fluorescence polarization technique.[13,29−32]

Preparation of Blend Samples. Miscible CA/vinyl polymer films were cast from mixed polymer solutions by solvent evaporation. DMF was selected as a common solvent. A 5.0 wt % solution of CA and that of the vinyl polymer as a counter component were prepared separately and mixed with each other in the desired weight proportions. After stirring over a period of 24 h at room temperature (25 °C), a small quantity of solution of BBS in DMF was added into the blend solutions so that the concentration of the fluorescent probe in each cast film was able to reach $\sim 5.0 \times 10^{-5}$ mol/L, and then the blend solutions were further stirred overnight. At this level of BBS concentration, any effect of fluorescence depolarization, caused by energy migration due to higher concentration of chromophores, is substantially negligible.[13,31,33] Both blend and plain

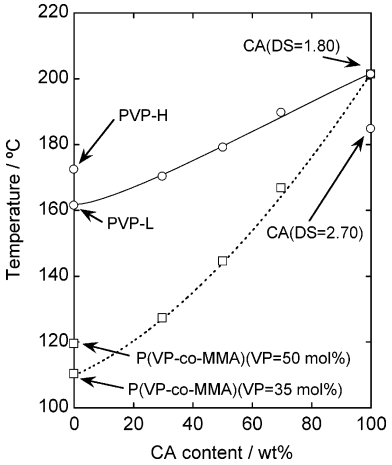

Figure 3. Representative plots of T_g vs CA content for CA blends with PVP or P(VP-*co*-MMA) copolymer. T_g was determined from the midpoint of a baseline shift appearing in the respective DSC thermograms.

polymer films ca. 100 μm thick were made on a Teflon tray via casting the respective solutions at 50 °C under reduced pressure. Strips of 20 × 4 mm cut from the as-cast films were dried at 40 °C in vacuo for 3 days, followed by further heat treatment at 120 °C in vacuo for 10 min.

Each of the film strips was fixed onto a hand-cranked drawing device which was allowed to be placed in a heated air oven. Then the film was uniaxially stretched to the desired draw ratio at a temperature which was prescribed to be higher by 2 °C than the glass transition point (T_g) of the blend or unblended sample used. The deformation rate was ∼45 mm/min. After the drawing process was completed, the film specimens were cooled quickly to ambient temperature (25 °C) and then stored in a desiccator until used for the measurements. The draw ratio (λ) or percentage elongation (ϵ) [$\epsilon = (\lambda - 1) \times 100\%$] of the oriented samples was determined from the positions of ink marks on the films.

Measurements. Differential scanning calorimetry (DSC) was conducted with a Seiko DSC6200/EXSTAR6000 apparatus to determine the glass transition temperature (T_g) of the respective film samples to be elongated. The scanning procedure and condition were the same as those adopted previously.[24,27] The thermogram of the second heating scan was employed for the T_g determination. In Figure 3, typical plots of T_g vs CA content are illustrated for representative samples; T_gs of the miscible blends are found to be widely changeable depending on the DS of CA, molecular weight of PVP, and VP:MMA ratio in P(VP-*co*-MMA). On the basis of these T_g data, the temperature of drawing for the respective films was prescribed.

Fluorescence polarization measurements allow the determination of the second and fourth moments of the orientation distribution function. The measurements were performed at ambient temperature (20 °C) with an apparatus that had been built in our laboratory.[13]

When the alignment of the molecular axis (**M**-axis) of a fluorescent probe is specified by a set of polar and azimuthal angles (ω, φ) in a sample coordinate system *O*-*XYZ*, where the *Z*- and *Y*-axes are aligned in the draw direction of a film sample and in the direction perpendicular to the plane of the film surface, respectively, the molecular orientation state can be characterized statistically in terms of the second and fourth moments defined in the following way:

$$\langle \cos^k \omega \rangle = \int_0^{2\pi} \int_0^{\pi} \cos^k \omega N(\omega,\varphi) \sin \omega \, d\omega \, d\varphi \quad (k = 2, 4) \tag{1}$$

where $N(\omega,\varphi)$ is a normalized function representing the molecular orientation distribution. According to the procedure established formerly by Nishio et al.,[13] the values of $\langle \cos^2 \omega \rangle$ and $\langle \cos^4 \omega \rangle$ can be determined from eqs 2 and 3, respectively.

$$\langle \cos^2 \omega \rangle = \left[\frac{2(A^2+2)}{3A-1} \middle/ \left\{ 2(A+2) - \frac{3I_{zz} - 8I_{xx}}{I_{zz} + 2I_{zx}} \right\} \right] + \frac{A-1}{3A-1} \tag{2}$$

$$\langle \cos^4 \omega \rangle = \frac{4}{(3A-1)^2} \left\{ \frac{A(3A-1)}{2} \langle \cos^2 \omega \rangle - \frac{A^2-1}{4} - \frac{(3A-1)\langle \cos^2 \omega \rangle - (A-1)}{(I_{zz}/I_{zx}) + 2} \right\} \tag{3}$$

where I_{ij} ($i, j = X$ or Z) is a polarized component of the fluorescence intensity and A is a parameter that characterizes the intrinsic photophysical anisotropy of the fluorescent molecule which is dispersed as an orientation probe in a polymeric medium. Four polarized components, I_{zz}, I_{zx}, I_{xx}, and I_{xz}, were measured by using the following combinations of the transmission axis of a polarizer and that of an analyzer: let I_{zz} be a polarized component of the fluorescence intensity which is observed when the two axes are both parallel to the *Z*-axis and I_{zx} be a component obtained when the axis of the polarizer and that of the analyzer are parallel to the *Z*- and *X*-axes, respectively. I_{xx} and I_{xz} can be defined in a similar way. For the stilbene derivative BBS, the anisotropy of light absorption and that of emission were assumed to be similar in extent, since the observed intensities I_{zx} and I_{xz} were almost equal to each other irrespective of the degree of orientation of the actually drawn samples.[13] Then the value of A can be obtained from the following relationship applicable to undrawn samples with a random orientation distribution:

$$\frac{I_{zz} - I_{zx}}{I_{zz} + 2I_{zx}} = \frac{2}{5}\left(\frac{3A-1}{2}\right)^2 \tag{4}$$

Ideally the A value is 1, if both light-absorbing axis and emitting one of the fluorescent probe coincide with the molecular axis **M** to be a single linear oscillator. However, it is usually less than 1 due to some effects involving thermal fluctuations in structure of the molecule. In the present study, the value was ∼0.83 as an average.

The birefringence (Δn) of drawn CA/vinyl polymer samples was determined by using an Olympus polarized optical microscope POS equipped with a Berek compensator, at room temperature (20 °C). The thickness of each film specimen was measured separately with a dial gauge.

Results and Discussion

1. CA/PVP Blends. The visual inspection and thermal transition behavior of a series of CA blends with a lower molecular-weight PVP-L have already been described in a previous paper.[24] In brief, the blend films employing CAs of DS < 2.75 were homogeneous and highly transparent, and the thermograms gave a single, composition-dependent T_g (see Figure 3). Even when a higher molecular-weight PVP-H was blended with the CAs, the thermal behavior of the blends was almost similar, but their T_gs elevated by less than 10 °C relative to those of the corresponding CA/PVP-L compositions. Thus, all the CA/PVP pairs used in this paper provided miscible blend films over the entire range of binary compositions.

1.1. Molecular Orientation Characteristics. In Figure 4, the second moment of molecular orientation, $\langle \cos^2 \omega \rangle$, evaluated by the fluorescence polarization method, is plotted against the percentage elongation of film specimens of CA(DS = 2.18)/PVP-H blends. Generally, films of unblended CA, the DS ranging from 1.80 to 2.70, showed quite a high level of molecular orientation on stretching; however, they were prone to break at an earlier stage of elongation (ϵ = ∼50%). The capability of CA for high degrees of orientation may be attributed not only to the relatively semirigid carbohydrate backbone but also to the intermolecular interactions via hydrogen-

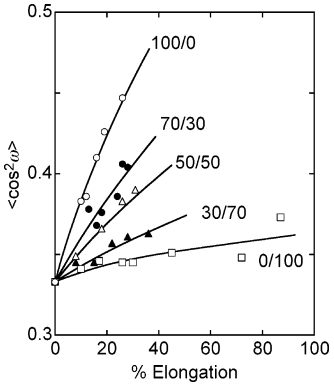

Figure 4. Plots of $\langle\cos^2\omega\rangle$ vs % elongation for drawn blends of CA-(DS = 2.18)/PVP-H.

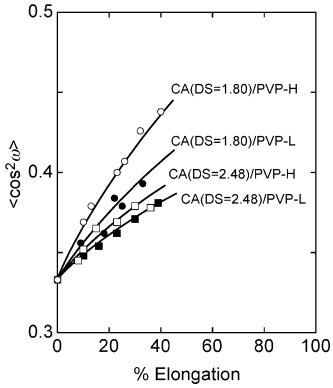

Figure 5. Plots of $\langle\cos^2\omega\rangle$ vs % elongation for selected CA/PVP blends which were prepared at a 70/30 composition.

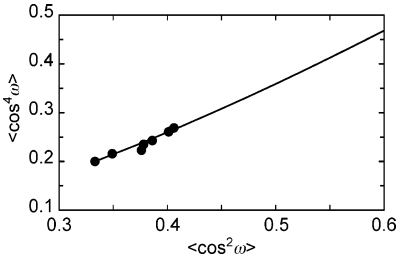

Figure 6. Plots of $\langle\cos^4\omega\rangle$ vs $\langle\cos^2\omega\rangle$ for drawn CA(DS = 2.18)/PVP-H samples with a 70/30 composition. The continuous line represents a relationship between the two moments calculated in terms of a model of prolate ellipsoid of rotation for the type of molecular orientation distribution.

bonding between the residual hydroxyl groups. As is made clearer in a later discussion, actually, the values of $\langle\cos^2\omega\rangle$ for plain CA films decreased slightly with increasing DS value, when compared at a given draw ratio, possibly due to the decrease in frequency of the hydrogen-bonding interactions. On the other hand, a considerably lower level of orientation prevailed in drawn PVP films, as seen in Figure 4. This vinyl polymer material is known to be highly susceptible to plastic flow during deformation at T_g and higher temperatures;[13] a rapid orientation relaxation concurrent in the drawing process may be responsible for the inherently less capability for orientation. In support of this idea, drawn PVP-H films gave somewhat higher values of $\langle\cos^2\omega\rangle$ than PVP-L films at every stage of elongation, since the PVP-H molecules of longer chain length have longer relaxation times. It should be kept in mind, however, that both PVP films imparted a decidedly "positive" orientation function, i.e., $f = (3\langle\cos^2\omega\rangle - 1)/2 > 0$, on stretching.

Concerning the blends of CA and PVP(-L or -H), the $\langle\cos^2\omega\rangle$ vs percentage elongation plots were always located between the corresponding plots obtained for the two polymers per se. Namely, the degree of orientation decreased monotonically with an increase in PVP content, when compared at a given stage of elongation. A similar composition dependence of the molecular orientation was observed for all the blend series of CA/PVP examined, irrespective of the DS of CA and the molecular weight of PVP. In the previous papers[24,25] dealing with the miscibility of CA and PVP, we reported the presence of a specific intercomponent interaction, i.e., the hydrogen bonding which was formed between the residual hydroxyls of CA and the carbonyls of VP units, as a driving force for attainment of the blend miscibility. Owing to the attractive interaction, presumably, the two polymers must have been oriented cooperatively in the blend films during the course of the uniaxial stretching process.

Figure 5 shows data of $\langle\cos^2\omega\rangle$ vs percentage elongation for four selected CA/PVP blends with a fixed composition of 70/30, prepared by using combinations of DS = 1.80 or 2.48 and PVP-L or -H. As can be seen from the comparison between the four sets of the plot, the selection of the lower DS of CA and that of the higher molecular weight of PVP result in the attainment of a higher degree of molecular orientation. It is conceivable that the molecular mobility and orientation relaxation are more limited in the more viscous polymer medium which contains the PVP species of a higher molecular weight. Furthermore, both lower DS of CA and higher molecular weight of PVP would increase the number of the functional groups associated with the hydrogen bonding, per unit molecule of the respective polymers, which allows the blend matrix to be a "quasi-network system" having a higher density of cross-links. This is also in favor of a restriction of the possible relaxation of the molecular orientation in the deformed polymer blends. A similar consideration has been made in an orientation study for a miscible poly(vinyl alcohol)/PVP system.[13]

In the fluorescence polarization method, it is possible to obtain information about not only the degree but also the type of molecular orientation in the noncrystalline regions of polymer solids.[13,29−32] A convenient way for estimating the type of molecular orientation is to construct a plot of the fourth moment $\langle\cos^4\omega\rangle$ against the second moment $\langle\cos^2\omega\rangle$ of orientation and then to search for conformity of the plot to a theoretical relationship between the moments calculated in terms of some potential model of the orientation distribution. Figure 6 exemplifies the construction of the $\langle\cos^4\omega\rangle$ vs $\langle\cos^2\omega\rangle$ plot for a 70/30 composition of CA(DS = 2.18)/PVP-H blends. The continuous line in the figure represents a relationship derived by assuming that the molecular orientation obeys a type of prolate ellipsoid of rotation about the stretching axis of the film sample. The calculated curve is virtually equivalent to a theoretical curve predicted by a Kratky-type affine deformation scheme,[34] proposed for the orientation of rodlike structural units floating in a bulk matrix. As demonstrated in the figure, the experimental data obtained for all the drawn films of CA(DS = 2.18)/PVP-H = 70/30 fitted the calculated curve, implying that the type of molecular orientation distribution in the uniaxially deformed blend follows well the model of prolate ellipsoid of rotation regardless of the rate of orientation development. This held for the other series of CA/PVP blends examined, irrespective of the DS of CA, the PVP molecular weight, and the blend composition.

1.2. Optical Anisotropy Estimation. Optical birefringence derives from the orientation of polymer chains which have inherently the anisotropy of polarizability. In the simplest case of uniaxial stretching of amorphous homopolymers, the birefringence, defined as $\Delta n = n_{\parallel} - n_{\perp}$ with a refractive index ($n_{\parallel}$)

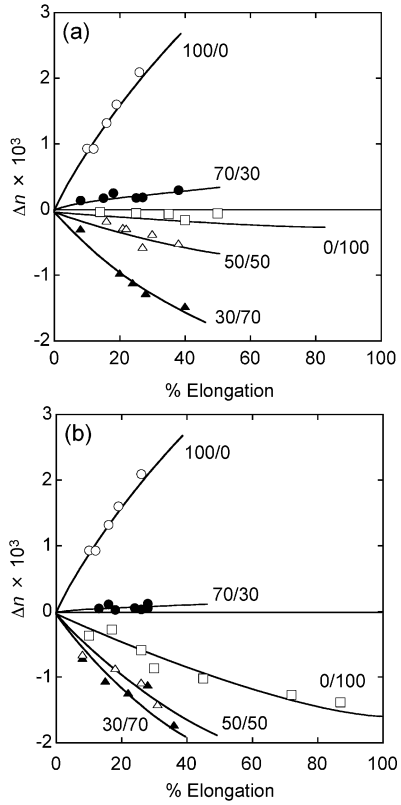

Figure 7. Plots of birefringence vs % elongation for drawn (a) CA(DS = 2.18)/PVP-L and (b) CA(DS = 2.18)/PVP-H.

parallel to the draw direction and that ($n_\perp$) perpendicular to it, can be given by

$$\Delta n = \frac{1}{2}(3\langle\cos^2\omega_s\rangle - 1)\Delta n^\circ \tag{5}$$

where Δn° is an intrinsic birefringence for the perfect uniaxial orientation of polymer chains and $\langle\cos^2\omega_s\rangle$ is the second moment of orientation for an anisotropic segmental unit **S** with a certain polarizability. Here it should be noted that two second moments, $\langle\cos^2\omega\rangle$ and $\langle\cos^2\omega_s\rangle$, obtained from the fluorescence polarization and birefringence measurements, respectively, are generally different in magnitude from each other, since there should be a respectable difference in size of the structural unit for orientation estimation between the two methods (usually $|\mathbf{S}| < |\mathbf{M}|$).

In the case of the stretching of a blend composed of polymer 1 and polymer 2, the birefringence Δn of the deformed sample may be represented by

$$\Delta n = v_1\Delta n_1 + v_2\Delta n_2 \tag{6}$$

where $v_i\Delta n_i$ ($i = 1, 2$) indicates the contribution of an oriented polymer component i to the total birefringence and v_i denotes the volume fraction of that component. If the sample contains a crystalline phase of a component i, Δn_i should be divided into two terms, taking account of the degree of crystallinity. In the present CA/PVP system, however, any of the blend samples can be assumed to be an overall amorphous material which exhibits a high level of miscibility.[24]

Parts a and b of Figure 7 show results of the birefringence measurements carried out on drawn CA(DS = 2.18)/PVP-L and CA(DS = 2.18)/PVP-H films, respectively. Unblended CAs of DS = 1.80−2.70 exhibited positive optical anisotropy ($\Delta n^\circ_{CA} > 0$) on stretching. However, the rise of Δn with percentage elongation was suppressed noticeably with increasing DS, which may be interpreted by assuming that the acetyl carbonyl groups aligned almost perpendicular to the cellulose backbone[1] compensate the optical anisotropy of the trunk polymer chain. On the other hand, as is already known,[13] drawn PVP films show a definitely negative birefringence ($\Delta n^\circ_{PVP} < 0$), notwithstanding the fact that the induced optical anisotropy is relatively low, particularly in the PVP-L samples.

Concerning the blends composed of the two polymers showing intrinsic birefringences of opposite sign, the following observations on the Δn data were worth noting, with respect to the dependence on the blend composition and that on the DS and molecular weight of the CA and PVP components, respectively.

(1) In all of the eight series of CA/PVP blends, Δn decreased monotonically but quite rapidly with increasing PVP content in the composition range 100/0−30/70, when compared at a given stage of elongation intermediate ca. 10 and 40%.

(2) At compositions containing ≥50 wt % PVP, drawn blends showed more negative birefringence than drawn, plain PVP. In the CA/PVP-L blends of acetyl DS ≥ 2.48, even the 70/30 films exhibited a smaller Δn (<0), compared with that of the PVP-L homopolymer samples deformed at similar draw ratios (data not shown).

(3) Any of the CA/PVP-H series gave lower Δn values, compared with the corresponding CA/PVP-L series; here, caution should be exercised to the fact that the former blend series was capable of higher orientation rather than the latter (e.g., see Figure 5).

(4) The higher the DS of the CA component, the wider was the composition range where drawn CA/PVP blends showed a negative birefringence.

In the present blend system, as is apparent from observations (1) and (2), there occurs a compensation effect due to the positive and negative contributions of the oriented CA and PVP, respectively, to the overall birefringence. Observation (3) indicates that the negative contribution of PVP is more intensely pronounced in the drawn blends containing higher-molecular-weight PVP. Observation (2) is also one of the pieces of evidence for a high level of miscibility in this blend system; because the result implies that orientation of the PVP molecules is appreciably enhanced in the presence of CA, possibly by virtue of the interpolymer interactions that occur through hydrogen bonding between the carbonyl and hydroxyl groups.

In correspondence with observations (3) and (4) stated above, a critical blend composition, conveniently defined as a minimal CA fraction, w_{1c}, below which the drawn blends show negative birefringence, would vary sensitively depending on the DS of the CA and on the molecular weight of the PVP component. To make it clearer, Figure 8 illustrates Δn vs CA content data obtained for four series of CA/PVP-H samples deformed to a draw ratio of ca. 1.25. For comparison, the composition dependence of Δn observed for a CA(DS = 1.80)/PVP-L series ($\epsilon = \sim 25\%$) is also represented by a dotted-line curve. It can readily be seen from the figure that the critical fraction w_{1c} for the two CA/PVP-H series using CAs of DS ≥ 2.48 is located between 0.70 and 1.00, while the fraction is rather lower ($0.50 < w_{1c} \leq 0.70$) in the case using CAs of DS ≤ 2.18. In addition, w_{1c} for the CA/PVP-L series is found to be further lower than that for the corresponding CA/PVP-H series. In the CA(DS = 1.80)/PVP-L series, w_{1c} is equal to ∼0.50, and actually the blend of 50/50 composition behaved as almost the birefringence-free material. Also, a 70/30 composition of CA(DS = 2.18)/PVP-H (i.e., $w_{1c} = 0.70$) was nearly the critical composition for the

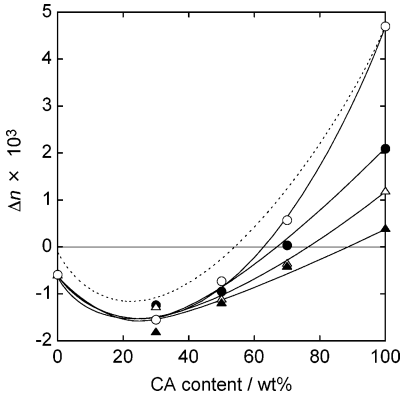

Figure 8. Birefringence vs blend composition for CA/PVP-H samples deformed uniaxially to a draw ratio of ~1.25. DS of CA: ○, 1.80; ●, 2.18; △, 2.48; ▲, 2.70. A dotted-line curve indicates, for comparison, a corresponding data obtained for a CA(DS = 1.80)/PVP-L series.

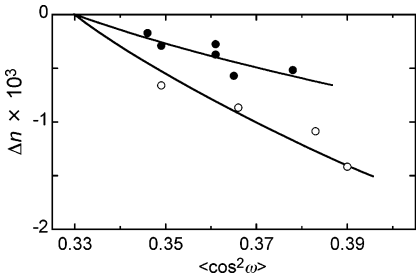

Figure 9. Birefringence vs $\langle\cos^2\omega\rangle$ for drawn blends of CA(DS = 2.18)/PVP-L (●) and CA(DS = 2.18)/PVP-H (○) with a 50/50 composition.

blend to be such a specific optical medium, as is evidenced by the Δn data in Figure 7b.

In Figure 9, Δn values are plotted as a function of the second moment of orientation for 50/50 compositions of the two series of CA(DS = 2.18)/PVP blends prepared with different PVP molecular weight. As is apparent from the comparison of the plots between the two series, even though the respective blends are oriented to an equal degree of $\langle\cos^2\omega\rangle$ when viewed in a structural unit of 2.5 nm scale, the CA/PVP-H series provides a negative birefringence greater in absolute value than that of the other series with PVP-L. This observation held true irrespective of the DS of the CA component. It follows, therefore, that the PVP-H component acquires a higher degree of orientation even at the segmental level in the drawn blends with CA and hence makes, more effectively, a negative contribution to the total birefringence, than does PVP-L when employed similarly.

2. CA/VP-MMA Copolymer Blends. Total six series of blend films composed CA and P(VP-*co*-MMA) copolymer were prepared so as to cover the miscible pairing region designated by the DS of CA and the VP fraction in P(VP-*co*-MMA), as indicated in Figure 2; CAs of DS = 1.80 and 2.18 were blended with the copolymers of VP = 35 and 47 mol %, and one more DS = 2.48 was combined with VP = 47 and 50 mol %. Any of the blend films showed a homogeneous, clear appearance, irrespective of the mixing polymer composition. In DSC measurements, these blends showed a noncrystalline nature and were confirmed to be miscible from the finding of a single, composition-dependent T_g that shifted to the higher temperature side along with increasing CA content (see Figure 3).

In Figure 10, the second moment of molecular orientation, $\langle\cos^2\omega\rangle$, measured for a series of blends of CA(DS = 1.80) with P(VP-*co*-MMA) of VP = 35 mol % are plotted against percentage elongation of the respective film specimens. Any

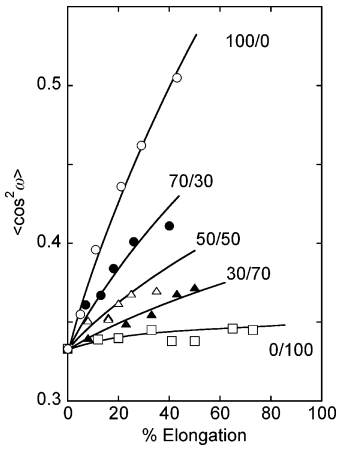

Figure 10. Plots of $\langle\cos^2\omega\rangle$ vs % elongation for CA(DS = 1.80)/P(VP-*co*-MMA)(VP:MMA = 35:65) blends.

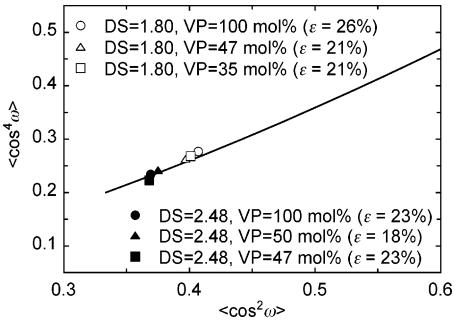

Figure 11. Plots of $\langle\cos^4\omega\rangle$ vs $\langle\cos^2\omega\rangle$ for selected samples of CA/P(VP-*co*-MMA) = 70/30 deformed uniaxially to a draw ratio of ca. 1.20−1.25. The acetyl DS and VP content of the CA and P(VP-*co*-MMA) components, respectively, are denoted in the figure. The solid-line curve indicates a theoretical relationship between the moments, the same as that depicted in Figure 6.

data point of the $\langle\cos^2\omega\rangle$ plot for each composition of the CA-(DS = 1.80)/copolymer blends was located at an equal or slightly lower level in the moment amplitude, compared with the data point obtained for the corresponding composition and elongation of the drawn blends of CA(DS = 1.80) with "PVP-H" (data not shown). A similar observation was made for the five series using the other combinations of the DS of CA and the VP:MMA ratio of P(VP-*co*-MMA). Here, it should be noted that the molecular weights of the copolymers used, ranging from 1.84×10^5 to 2.90×10^5, are considerably higher than that of PVP-L (2.45×10^4), but rather comparable to that of PVP-H (3.6×10^5).

Figure 11 exemplifies a construction of the $\langle\cos^4\omega\rangle$ vs $\langle\cos^2\omega\rangle$ plot for selected blends of CA(DS = 1.80 or 2.48) with PVP-H (VP = 100 mol %) and P(VP-*co*-MMA) of VP = 35−50 mol %, the film samples being deformed to a draw ratio of ca. 1.20−1.25 ($\epsilon \approx 20$−25%). The composition of CA/vinyl polymer is, in common, 70/30 in the weight proportion. A solid-line curve in the figure represents a theoretical relationship between the moments, calculated in terms of the ellipsoidal distribution model described in the preceding section. The $\langle\cos^4\omega\rangle$ vs $\langle\cos^2\omega\rangle$ data for three CA blends of DS = 1.80 are found on the solid-line curve, collecting at a comparatively higher level, while the data points for the other three of DS = 2.48 are closely situated on the curve at lower and left positions. Thus, in the uniaxial drawing of CA/P(VP-*co*-MMA) blends, the lower DS of the CA component is favorable for the progress in molecular orientation of the blends, but the variable VP:MMA ratio in the vinyl polymer is an inert factor scarcely affecting

the molecular orientation behavior in both degree and distribution type.

In the miscible CA/P(VP-*co*-MMA) system, the residual hydroxyls of CA form a hydrogen-bonding interaction with the carbonyls of the VP units in the vinyl copolymer, not with ones of the MMA units, as has already been proved in our previous paper.[27] Accordingly, the lower VP content in the copolymer would be of greater disadvantage for prevalence of a higher extent of orientation in the blends with CA due to the lower frequency of the intermolecular interaction, as does the higher DS of the CA component. In interpreting the less dependence of the orientation development in the CA/copolymer blends on the VP:MMA ratio, there is a possibility that the MMA segmental sequence may be essentially less susceptible of the orientation relaxation in the course of deformation of the vinyl polymer, rather than the VP sequence. In fact, some drawn films of PMMA ($M_w \approx 9 \times 10^4$) were prone to give a slightly higher degree of orientation than those of PVP-H, when compared at more than 100% elongation by the fluorescence polarization method, although both vinyl polymers showed an inherently less capability for orientation. Such an increased effect of relaxation restraint by the MMA units might have canceled out the less interaction effect attended by the decease of the VP content, when the CA/P(VP-*co*-MMA) blends were subjected to the uniaxial stretching.

Figure 12 compiles results of the birefringence measurements conducted for drawn films of three series of CA/P(VP-*co*-MMA) blends prepared with different combinations of DS and VP:MMA ratio: (a) DS = 1.80 and VP:MMA = 35:65; (b) DS = 2.18 and VP:MMA = 47:53; and (c) DS = 2.48 and VP:MMA = 50:50. As is well-known, drawn films of PMMA show negative optical anisotropy, a value of $\Delta n^\circ_{PMMA} = -50.7 \times 10^{-4}$ being predicted in the literature[35] as the intrinsic birefringence. Undoubtedly, therefore, the vinyl copolymer P(VP-*co*-MMA) should also give a negative birefringence on stretching the film, and in Figure 12, Δn data for the three samples designated commonly as 0/100 are actually consistent with this assumption.

The optical anisotropy of the oriented CA/P(VP-*co*-MMA) system was also affected seriously by the compensation effect due to the positive and negative contributions of the CA and copolymer components, respectively, to the overall birefringence, as can be seen from the swift change in location of the Δn vs percentage elongation plot with variation of the blend composition, observed for any of the three series in Figure 12. As shown in Figure 12b,c, some copolymer-rich blends provided a negative birefringence larger in magnitude than that of the respective unblended copolymers, reflecting a certain level of cooperative orientation of the miscible two polymer components in the uniaxial drawing process.

Comparing the birefringence data shown in Figure 12b for the CA(DS = 2.18)/P(VP-*co*-MMA)(VP:MMA = 47:53) series with those for the CA(DS = 2.18)/PVP-H series (Figure 7b), we find that the Δn values obtained for the 30/70, 50/50, and 70/30 compositions of the former series are higher than those for the corresponding compositions of the latter series at every stage of elongation. This observation was applicable to similar comparisons made between the respective two series of CA blends of other DSs with PVP-H and P(VP-*co*-MMA). In contrast, as mentioned previously, there was less difference in the extent of orientation development between the CA/VP-MMA copolymer and CA/PVP-H blends of a mutually equivalent binary composition, as far as a common CA was used. Therefore, we can readily infer from these results that the

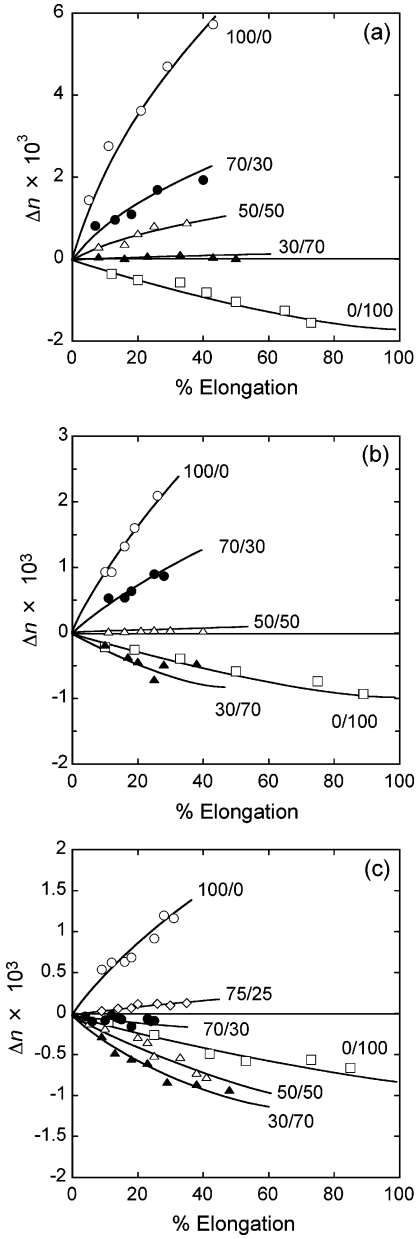

Figure 12. Birefringence vs % elongation for drawn films of three series of CA/P(VP-*co*-MMA) blends prepared with different combinations of DS and VP:MMA ratio: (a) DS = 1.80 and VP:MMA = 35:65; (b) DS = 2.18 and VP:MMA = 47:53; (c) DS = 2.48 and VP:MMA = 50:50.

negative contribution of PVP-H to the total birefringence is more intense than that of VP-MMA copolymers, implying that the negative anisotropy in polarizability of the VP unit is of greater extent than that of the MMA unit, i.e., $\Delta n^\circ_{PVP} < \Delta n^\circ_{PMMA}$. In correspondence to this, in the CA/copolymer series, the critical CA fraction w_{1c} at the composition to generate a zero-birefringence blend material is lowered to a considerable extent, compared with the corresponding CA/PVP-H series; for instance, in Figure 12b (DS of CA, 2.18), w_{1c} is found to be ~0.50 lowered from ~0.70 (see Figure 7b).

Of the three series shown in Figure 12, the combination (a) of DS = 1.80 and VP:MMA = 35:65 gives rise to the lowest critical value of w_{1c} = ~0.30 because this blend series is composed of a pair of CA having a positive Δn° of the largest magnitude and P(VP-*co*-MMA) having a negative Δn° of the smallest magnitude. As a matter of course, the highest w_{1c} value, a little over 0.70, can be observed for another CA/P(VP-*co*-

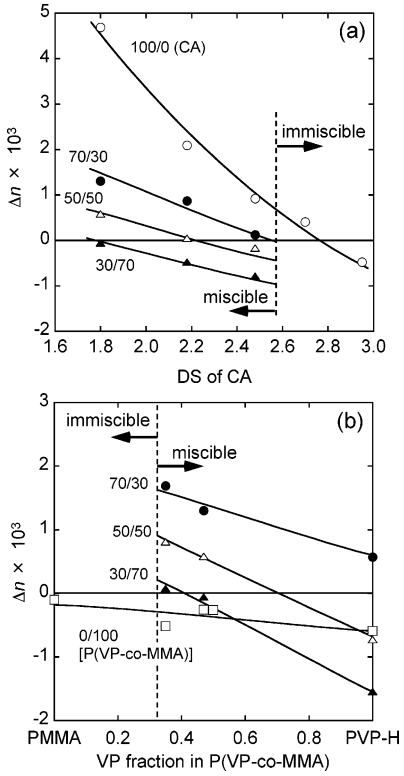

Figure 13. Birefringence for selected compositions of CA/P(VP-*co*-MMA) blends deformed to $\epsilon = \sim 25\%$, plotted as a function of (a) DS of CA and (b) VP fraction in P(VP-*co*-MMA), with the proviso that (a) VP:MMA = 47:53 and (b) DS = 1.80 for the respective blending partners.

MMA) series using the combination (c) of DS = 2.48 and VP:MMA = 50:50.

In Figure 13, Δn values are plotted as a function of (a) DS of CA and of (b) VP fraction in P(VP-*co*-MMA) for selected compositions of CA/P(VP-*co*-MMA) blends, with the proviso: (a) VP:MMA = 47:53 and (b) DS = 1.80 regarding the respective counterpart components. The film samples were all deformed to a draw ratio of ca. 1.25 ($\epsilon = \sim 25\%$). In Figure 13a, a birefringence data obtained for a CA of DS = 2.95 is also plotted for reference. This CA is a crystalline cellulose triacetate showing a negative Δn°, but it should be noted that CAs of DS $\geq$ 2.70 were immiscible with the VP−MMA copolymer. In the DS range ensuring the blend miscibility, we find a constant decrease of Δn with increasing acetyl DS for every composition, which is mainly ascribable to a decrease of the positive contribution of the CA component to the total birefringence, originating from the essentially declining amplitude of Δn°_{CA}. Focusing on another falling behavior of Δn attended by blending CA with the copolymer, the rate is generally greater at a lower DS of 1.80, compared with the situation at higher DSs. From this perspective, it can be said that the birefringence compensation effect is more accentuated in the CA(DS = 1.80) blends showing a comparatively higher degree of molecular orientation.

Figure 13b contains birefringence data obtained for unblended P(VP-*co*-MMA)s including PMMA (VP = 0 mol %) and PVP-H (VP = 100 mol %). Their films showed quite a low level of molecular orientation on stretching, and hence the resulting smaller Δn values (<0) bear less dependence on the VP:MMA ratio. The miscible blends with CA(DS = 1.80), however, make a linear relationship where Δn decreases remarkably with increasing VP fraction in P(VP-*co*-MMA), at any composition of 70/30−30/70. These blend samples showed an approximately equal degree of molecular orientation at each binary composition. Accordingly, that decrease just emphasizes the difference in the negative effectiveness of Δn° between the VP and MMA units in the vinyl polymer component which is better oriented by virtue of the miscible partner CA.

As is clearly demonstrated by both plots in Figure 13, the critical fraction w_{1c} to be observed for the miscible blends shifts to higher values with increasing DS of the CA component and with increasing VP fraction in the P(VP-*co*-MMA) component as well. In the miscibility map shown in Figure 2, three lines informing the critical binary composition are depicted, each designated as 70/30, 50/50, or 30/70. (In the line drawing, birefringence data for CA blends with "PVP-H" were involved.) The miscible polymer pairs with the DS and VP fraction coordinates fitting the respective lines can produce a birefringence-free material at the indicated blend composition. With the aid of this map, the optical anisotropy of the present system is desirably controllable by varying the binary polymer composition, as well as by altering the DS of CA and the VP:MMA ratio in P(VP-*co*-MMA), which is of great significance for designing some optically functional blend materials. In the case, however, attention should be paid to the possible change in hydrophilic/hydrophobic nature of the blends; generally, the hydrophobicity would escalate with the increase of the DS of CA and/or the MMA fraction in P(VP-*co*-MMA).

Conclusion

Blends of cellulose acetate (CA) with poly(*N*-vinylpyrrolidone) (PVP) and those with *N*-vinylpyrrolidone−methyl methacrylate (VP−MMA) random copolymer were prepared in clear film form by a solution-casting method, so that any pairing fulfilled the miscibility condition associated with the degree of substitution (DS) of the CA component and the VP:MMA ratio in the vinyl polymer [P(VP-*co*-MMA)] component. Eight series of CA/PVP blends using all combinations of four CAs of DS = 1.80−2.70 and two PVPs (PVP-L and -H, largely different from each other in molecular weight), and six series of CA/VP-MMA copolymer blends using selected combinations of three CAs of DS = 1.80−2.48 and three P(VP-*co*-MMA)s of VP = 35−50 mol % were examined for estimation of the molecular orientation and optical anisotropy, which were induced by drawing the film samples of different blend compositions uniaxially at the respective T_g + 2 °C. The estimation of molecular orientation was carried out by using the second ($\langle\cos^2 \omega\rangle$) and fourth ($\langle\cos^4 \omega\rangle$) moments, both obtained by the fluorescence polarization method.

All the dawn CA/vinyl polymer films imparted a positive orientation function ($\langle\cos^2 \omega\rangle > 0.33$) and an orientation distribution type of prolate ellipsoid of rotation around the stretching axis. The degree of molecular orientation decreased monotonically with an increase of the vinyl polymer content in the blends, when compared at an equal extent of elongation. In comparison between different series of CA/PVP blends, a series using lower-acetylated CA and PVP-H of higher molecular weight acquired a higher degree of orientation, relative to another series using higher acetylated CA and PVP-L of lower molecular weight, when examined at a given composition. The former blend series assuming a denser quasi-network is of greater advantage to restriction of the possible relaxation of the molecular orientation in the deformation process. Concerning the CA/VP−MMA copolymer series, the selection of a lower DS for the CA component was in favor of a better progress of the molecular orientation in the drawn films, similar to the situation in the CA/PVP series; however, the dependence of

the orientation on the VP:MMA ratio of the copolymer component was less prominent. Virtually, the orientation behavior in the CA/VP−MMA copolymer blends was nearly the same as that in the corresponding CA blends with PVP-H having a molecular weight comparable to those of the copolymers used.

The two-component polymers CA and P(VP-*co*-MMA) constituting the present system showed a mutually opposite sign in the intrinsic birefringence, and the drawing of the blend films gave rise to a characteristic change in the optical anisotropy with composition. The overall birefringence (Δn) of the drawn blends, when compared at a given stage of elongation, decreased rapidly with a decrease in the CA fraction (w_1) until w_1 reached a certain value (w_{1c}) at which Δn changed from positive to negative. This reflects well a compensation effect due to the positive and negative contributions of the cellulosic and vinyl polymer components, respectively, to the total birefringence of the blends. In several blend series, at vinyl polymer-rich concentrations, the negative birefringence observed for the drawn blends was greater in absolute value than that of the drawn, plain vinyl polymer. This observation strongly suggests that the two constituent polymers can orient cooperatively to a considerable extent as a result of their miscibility at the molecular level. For detailed elucidation of the molecular orientation in the blend system, however, it should be necessary to estimate the individual orientation behavior of the two polymer components. In this work, the behavior of the blends was discussed solely on the basis of comparison in terms of two "average" orientation parameters, obtained by fluorescence and birefringence methods. Further characterization by other techniques including infrared dichroism measurements[36−38] remains to be reported in the near future.

The binary composition range where the drawn blends show a negative birefringence is expanded by any of the ascents of the following parameters: DS of CA, molecular weight of PVP, and VP fraction in P(VP-*co*-MMA). In a miscibility map for the present blend system, constructed as a function of the acetyl DS and VP fraction characterizing the two components, we successfully made a plot informing the critical binary composition at which a given polymer blend shows a zero-birefringence nature, irrespective of the draw ratio of the film or the degree of molecular orientation which is induced. Thereby, it is possible to control desirably the optical anisotropy of the oriented, miscible polymer system. The present result may be useful for designing new optical materials based on CA or MMA-containing polymers.

References and Notes

(1) Sata, H.; Murayama, M.; Shimamoto, S. *Macromol. Symp.* **2004**, *208*, 323.
(2) Nakayama, H.; Fukagawa, N.; Nishiura, Y.; Yasuda, T.; Ito, T.; Mihayashi, K. *J. Photopolym. Sci. Technol.* **2006**, *19*, 169.
(3) Iwata, S.; Tsukahara, H.; Nihei, E.; Koike, Y. *Jpn. J. Appl. Phys.* **1996**, *35*, 3896.
(4) Tagaya, A.; Ohkita, H.; Harada, T.; Ishibashi, K.; Koike, Y. *Macromolecules* **2006**, *39*, 3019.
(5) Tagaya, A.; Iwata, S.; Kawanami, E.; Tsukahara, H.; Koike, Y. *Jpn. J. Appl. Phys.* **2001**, *40*, 6117.
(6) Ohkita, H.; Ishibashi, K.; Tsurumoto, D.; Tagaya, A.; Koike, Y. *Appl. Phys. A: Mater. Sci. Process.* **2005**, *81*, 617.
(7) Koike, Y.; Yamazaki, K.; Ohkita, H.; Tagaya, A. *Macromol. Symp.* **2006**, *235*, 64.
(8) Tagaya, A.; Ohkita, H.; Koike, Y. *Mater. Sci. Eng., C* **2006**, *26*, 966.
(9) Hahn, B. R.; Wendorff, J. H. *Polymer* **1985**, *26*, 1619.
(10) Saito, H.; Inoue, T. *J. Polym. Sci., Part B: Polym. Phys.* **1987**, *25*, 1629.
(11) Zhao, Y.; Jasse, B.; Monnerie, L. *Polymer* **1991**, *32*, 209.
(12) Nishio, Y.; Haratani, T.; Takahashi, T. *J. Polym. Sci., Part B: Polym. Phys.* **1990**, *28*, 355.
(13) Nishio, Y.; Suzuki, H.; Sato, K. *Polymer* **1994**, *35*, 1452.
(14) Nishio, Y. In *Cellulosic Polymers, Blends and Composites*; Gilbert, R. D., Ed.; Hanser Pub.: Munich, 1994; Chapter 5, p 95.
(15) Nishio, Y. *Adv. Polym. Sci.* **2006**, *205*, 97.
(16) Buchanan, C. M.; Gardner, R. M.; Komarek, R. J. *J. Appl. Polym. Sci.* **1993**, *47*, 1709.
(17) Komarek, R. J.; Gardner, R. M.; Buchanan, C. M.; Gedon, S. *J. Appl. Polym. Sci.* **1993**, *50*, 1739.
(18) Shibata, T. In *The Recent Trends of Glycochemistry*; Kobayashi, K., Shoda, S., Eds.; CMC Pub.: Tokyo, 2003; Part 2, p 121.
(19) Teramoto, Y.; Nishio, Y. *Polymer* **2003**, *44*, 2701.
(20) Teramoto, Y.; Nishio, Y. *Biomacromolecules* **2004**, *5*, 397.
(21) Teramoto, Y.; Nishio, Y. *Biomacromolecules* **2004**, *5*, 407.
(22) Teramoto, Y.; Ama, S.; Higeshiro, T.; Nisho, Y. *Macromol. Chem. Phys.* **2004**, *205*, 1904.
(23) Nishio, Y.; Matsuda, K.; Miyashita, Y.; Kimura, N.; Suzuki, H. *Cellulose* **1997**, *4*, 131.
(24) Miyashita, Y.; Suzuki, T.; Nishio, Y. *Cellulose* **2002**, *9*, 215.
(25) Ohno, T.; Yoshizawa, S.; Miyashita, Y.; Nishio, Y. *Cellulose* **2005**, *12*, 281.
(26) Ohno, T.; Nishio, Y. *Cellulose* **2006**, *13*, 245.
(27) Ohno, T.; Nishio, Y. *Macromol. Chem. Phys.* **2007**, *208*, 622.
(28) Liu, Y.; Huglin, M. B.; Davis, T. P. *Eur. Polym. J.* **1994**, *30*, 457.
(29) Nishijima, Y. *J. Polym. Sci., Part C* **1970**, *31*, 353.
(30) Nishijima, Y. In *Progress in Polymer Science, Japan*; Onogi, S., Uno, K., Eds.; Kodansha: Tokyo, 1973; Vol. 6, p 199.
(31) Nishio, Y.; Tanaka, H.; Onogi, Y.; Nishijima, Y. *Rep. Progr. Polym. Phys. Jpn.* **1979**, *22*, 469.
(32) Murase, S.; Hirami, M.; Nishio, Y.; Yamamoto, M. *Polymer* **1997**, *38*, 4577.
(33) Pucci, A.; Bertoldo, M.; Bronco, S. *Macromol. Rapid Commun.* **2005**, *26*, 1043.
(34) Kratky, O. *Kolloid Z.* **1933**, *64*, 213.
(35) Zhao, Y.; Jasse, B.; Monnerie, L. *Makromol. Chem., Macromol. Symp.* **1986**, *5*, 87.
(36) Lefebvre, D.; Jasse, B.; Monnerie, L. *Polymer* **1981**, *22*, 1616.
(37) Bouton, C.; Arrondel, V.; Rey, V.; Sergot, Ph.; Manguin, J. L.; Jasse, B.; Monnerie, L. *Polymer* **1989**, *30*, 1414.
(38) Zhao, Y.; Prud'homme, R. E.; Bazuin, C. G. *Macromolecules* **1991**, *24*, 1261.

MA062920T